Electronic Supplementary Information

1) Photonic crystals preparation

Titania and silica mesoporous thin films were deposited on glass by spin coating, using a combination of sol-gel process and evaporation induced self-assembly of surfactants under controlled conditions [1].

Three different templates were used, non-ionic triblock copolymer Pluronic F127 ($[EO]_{106}[PO]_{70}[EO]_{106}$; EO = ethylene oxide, PO: propylene oxide), non-ionic surfactant Brij-58 ($C_{16}H_{33}(EO)_{20}OH$) and cationic surfactant CTAB ($C_{16}H_{33}N(CH_3)_3Br$).

$TiCl_4$ and $Si(OEt)_4$ (Et=ethyl) were used as inorganic precursors. In the case of titania films, the ethanolic solution contains a proportion $TiCl_4$:template:H_2O:EtOH with 1:s:10:80 molar ratio, where s = 0.005 for F127 and s = 0.05 for Brij-58.

For the production of silica films, a prehydrolysis was prepared by refluxing $Si(OEt)_4$ for 1 h in a water-ethanol solution, with $[H_2O]/[Si]$ = 1 and $[EtOH]/[Si]$ = 5. Silica solutions were produced then using a TEOS:EtOH:H_2O (0.1M HCl) mixture, with 1:40:5 ratio; the reagents were stirred at 60°C for 1 h prior to spin or dip-coating. This prehydrolysed solution was then used to prepare 2 different sols with CTAB and Brij58 as surfactants. These sols were comprised of $Si(OEt)_4$:template:H_2O:EtOH:HCl with a molar ratio 1:s:h:40:p, where s=0.1, h=5, p=0.004 for the sol with CTAB as template and s=0.05, h=10 and p=0.008 for the sol with Brij58.

8-layered distributed Bragg reflectors (DBRs) were synthesized by the alternate deposition of titania and silica mesoporous films on glass substrates, using a spin-coater or a dip-coater [1-3]. To control the thickness of each DBR layer, the deposition velocity for dip-coated films was tuned between 0.6 and 1.5 mm s^{-1} (withdrawal speed) and for spin-coated films, from 1600 to 3000 rpm (spin speed). The DBRs were called 4x(SX/TX), were S is silica, T is titania, and X is the surfactant used to obtain the mesoporous structure; F for Pluronic F127, B for Brij58 and C for CTAB.

After each film deposition, two different thermal treatments were carried out to stabilize and consolidate the oxide walls. Dip-coated films were submitted to a 50% RH chamber for 24 h and subsequently treated at 60°C and 130°C for 24 h; to consolidate the mesoporous layer, they were treated at 200°C for 2 h. Finally, the obtained DBRs were calcined at 350°C for 2 h (ramp 1°C min^{-1}) to eliminate the template. Spin-coated films were submitted to a similar consolidation treatment but each step was 30 min long; the multi-layered structures obtained were calcined for 2 h at 300°C (ramp 1°C min^{-1}).

2) Optical simulations and characterization

Simulation of the optical properties of the devices: Numerical simulations were performed using a standard transfer-matrix method[4, 5]. The device is represented as a stack of ideal layers of defined thicknesses and refractive indexes. The substrate was treated as a semi-infinite medium. The PL layer was modelled as an additional thin film

on top of the stack. A constant and real refractive index was used for the dielectric layers, with values; 1.5 for glass substrate, 1.28 for porous SiO_2 and 1.72 for porous TiO_2 [3] while wavelength-dependent values for the dielectric function of the Au, Ti and Cr layers were taken from literature[6]. Several devices were modelled and the results are presented in **Figure S1**:

1) a DBR, consisted of a stack of 4 SiO_2-TiO_2 bilayers on glass; the medium above the device was air (n=1); each DBR layer has a thickness $t_i = \lambda_0/4/n_i$, being λ_0 the position of the DBR stop band (centered at λ_0=600 nm in this case), and n_i the refractive index for the corresponding layer;

2) a TPP device, consisted of the DBR followed by a 20 nm thick gold layer;

3) a TTP device capped by a 20 nm thick PL with n=1.75;

4) a DBR capped by a 5 nm thick adhesion layer (Ti or Cr) followed by the 20 nm thick Au layer.

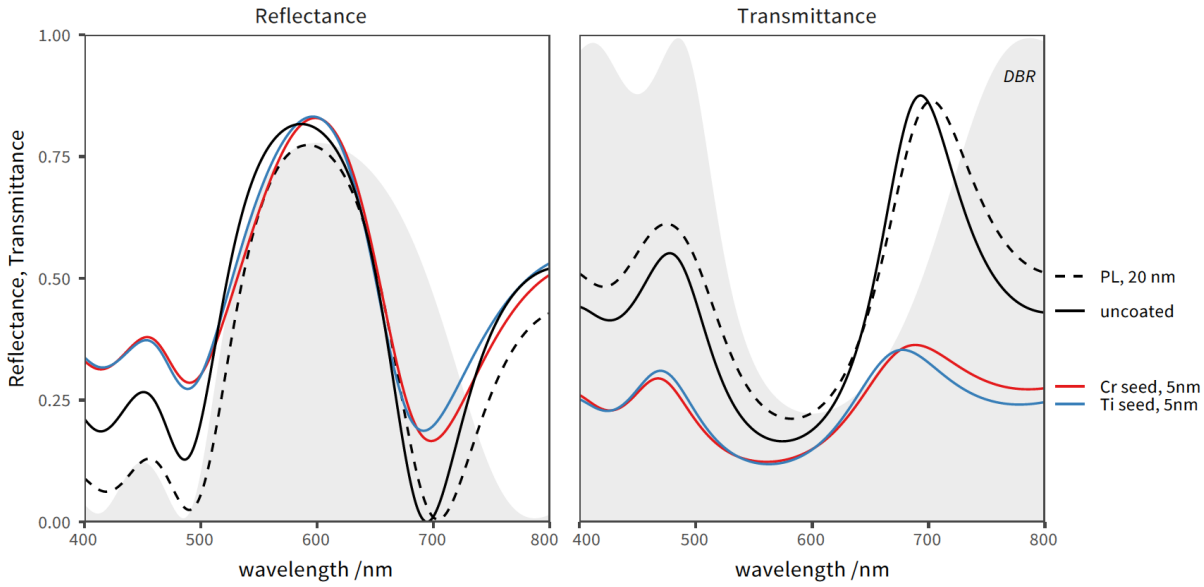

Figure S1. Simulated reflectance (left) and the transmittance (right) spectra of a Tamm plasmon device both uncoated (black solid line) and coated with a superficial 20 nm thick PL (black dashed line). The grey shadows represent the corresponding DBR spectra (i.e. the device without the Au layer). The simulated spectra obtained using a 5 nm thick Ti (blue line) and 5 nm thick Cr (red line) adhesion layers between the DBR and the Au layer are also presented.

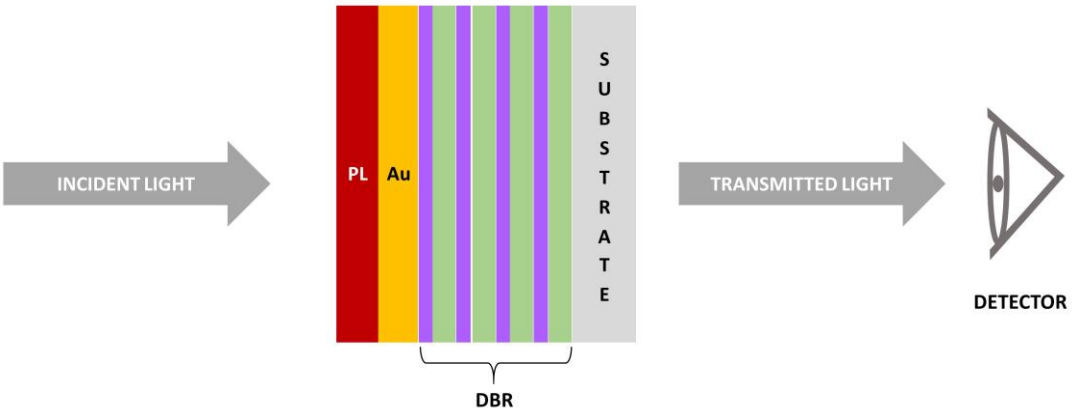

Figure S2. Scheme of the experimental setup used for transmission measurements. Drawn not to scale.

3) PL structural characterization

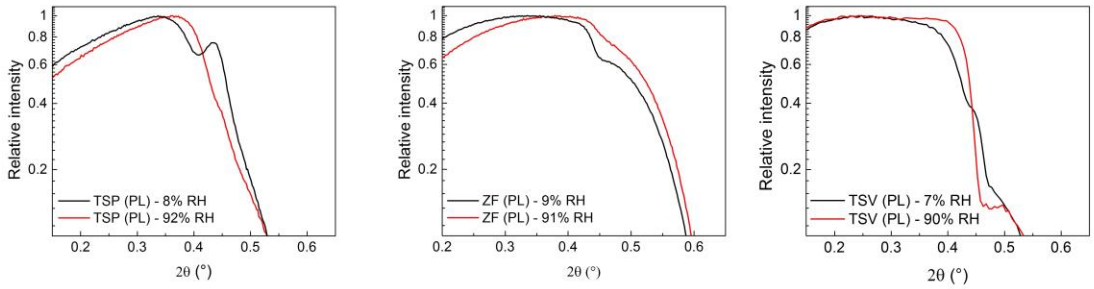

Figure S3. XRR patterns (critical angle region) of PLs measured at low and high relative humidity (RH), from which the accessible porosities were calculated: (16 ± 3)% for TSP; (30 ± 8)% for ZF and (15 ± 3)% for TSV.

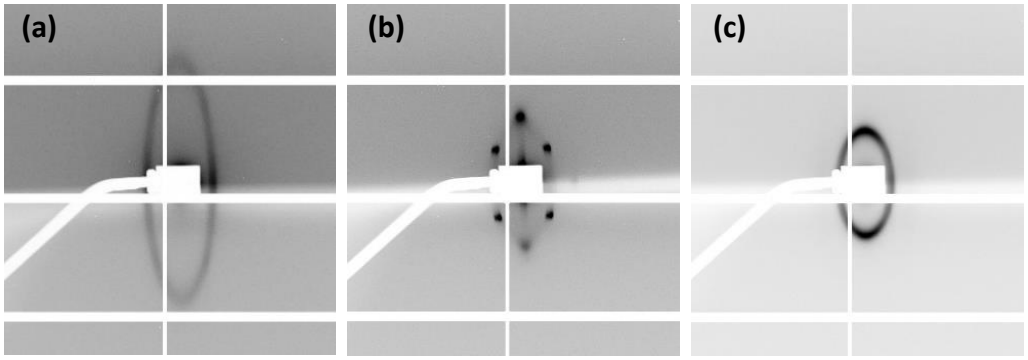

Figure S4. SAXS patterns obtained for **(a)** ZF, **(b)** TSP and **(c)** TSV samples.

4) PL mechanical characterization

a) Nanoindentation measurements

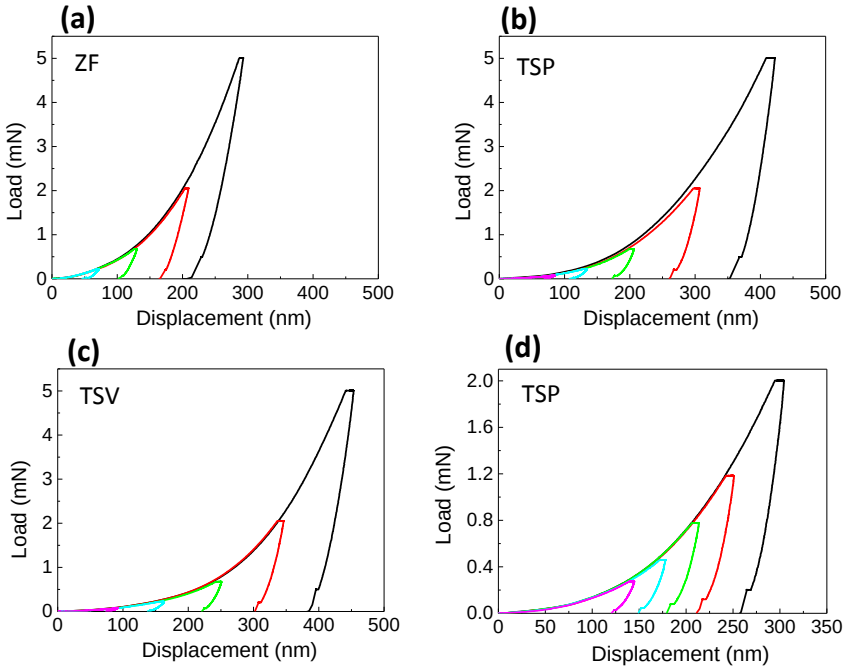

Figure S5. Load vs displacement measurements (ISO method) for **(a)** ZF (300°C), **(b)** TSP (200°C) and **(c)** TSV (200°C) up to a maximum load of 5 mN. **(d)** Load vs displacement measurements for TSV (200°C) up to a maximum load of 2 mN.

b) Calculation of E_{IT} and H_{IT} from load vs displacement measurements

Oliver & Pharr method was used to get E_{IT} and H_{IT} from each load-displacement curve [7]. Power law fit is used to calculate stiffness (S) evaluated at the beginning of the unloading response. Contact depth (h_c) is obtained from the following equation:

$$h_c = h_m - \varepsilon\left(\frac{P_m}{S}\right)$$

Here, h_m is indentation maximum depth, ε is a constant that depends on tip geometry and P_m is the maximum load applied. Contact area (A) is determined applying the area function (F), which is defined during tip calibration, at h_c value

$$A = F(h_c)$$

The reduced elastic modulus (E_r) was calculated according to the following equation:

$$E_r = \frac{\sqrt{\pi}}{2\beta}\frac{S}{\sqrt{A}}$$

β is a geometrical factor, being 1.034 the most commonly used for a Berkovich tip [8]. Sample modulus (E_{IT}) is calculated according to

$$\frac{1}{E_r} = \left(\frac{1-\nu^2}{E_{IT}}\right) + \left(\frac{1-\nu_i^2}{E_i}\right)$$

where ν is sample Poisson's ratio, E_i and ν_i are indenter elastic modulus and Poisson's ratio (E_i =1141 GPa y ν_i = 0,07 for a diamond tip).
On the other hand, H_{IT} is obtained from the ratio between P_m and A.

$$H_{IT} = \frac{P_m}{A}$$

To obtain the mechanical properties of thin films, indentations were made at different depths (load control, up to decreasing maximum loads). The calculated H_{IT} values for each penetration tested were then plotted as a function of the parameter h_c/t_c; the E values, as a function of the parameter a/t_c, being a the radius of the projected area, h_c the contact depth and t_c the film thickness, as defined by the ISO 14577 method (https://www.iso.org/ standard/61823.html) (see **Figure S5**). Then, extrapolations are made for h_c/t_c = 0 (fitting range 0 < h_c/t_c < 1) and a/t_c = 0 (fitting range 0 < a/t_c < 2) to obtain H_{IT} and E_{IT} of the films, respectively.
The same procedure was applied to calculate E_{IT} and H_{IT} from measurements up to 2 mN. The final values reported in **Table 1** are the average of the values calculated from the measurements performed at 2 and 5 mN maximum load.

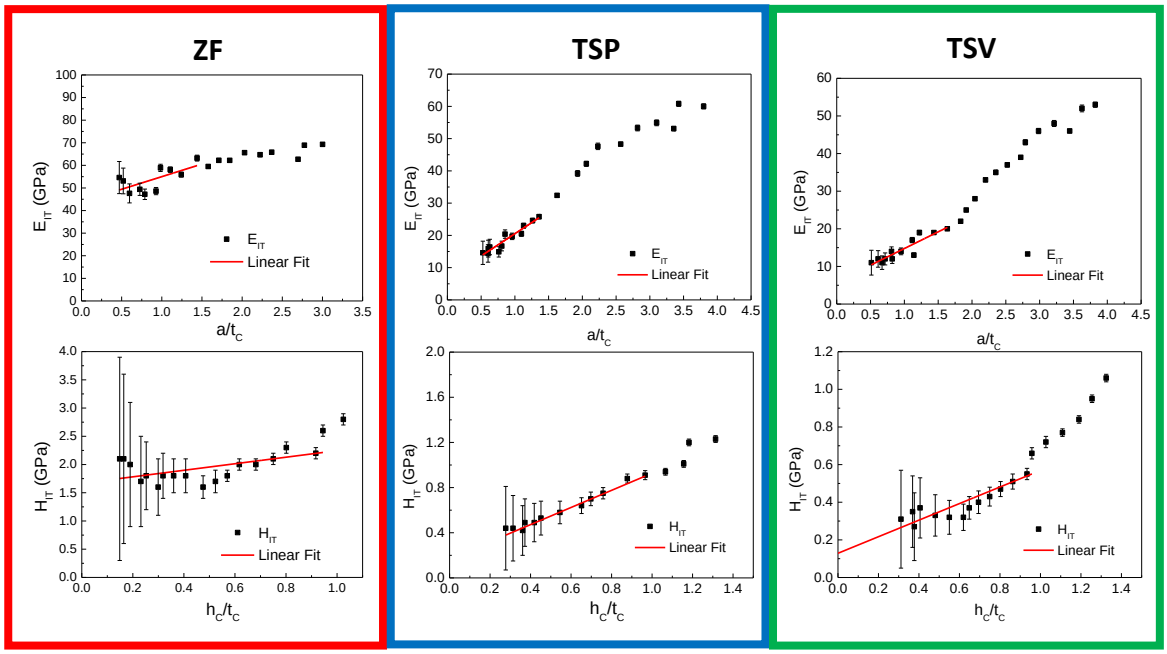

Figure S6. Calculation of E_{IT} and H_{IT} from measurements up to 5 mN (ISO method).

c) Scratch tests

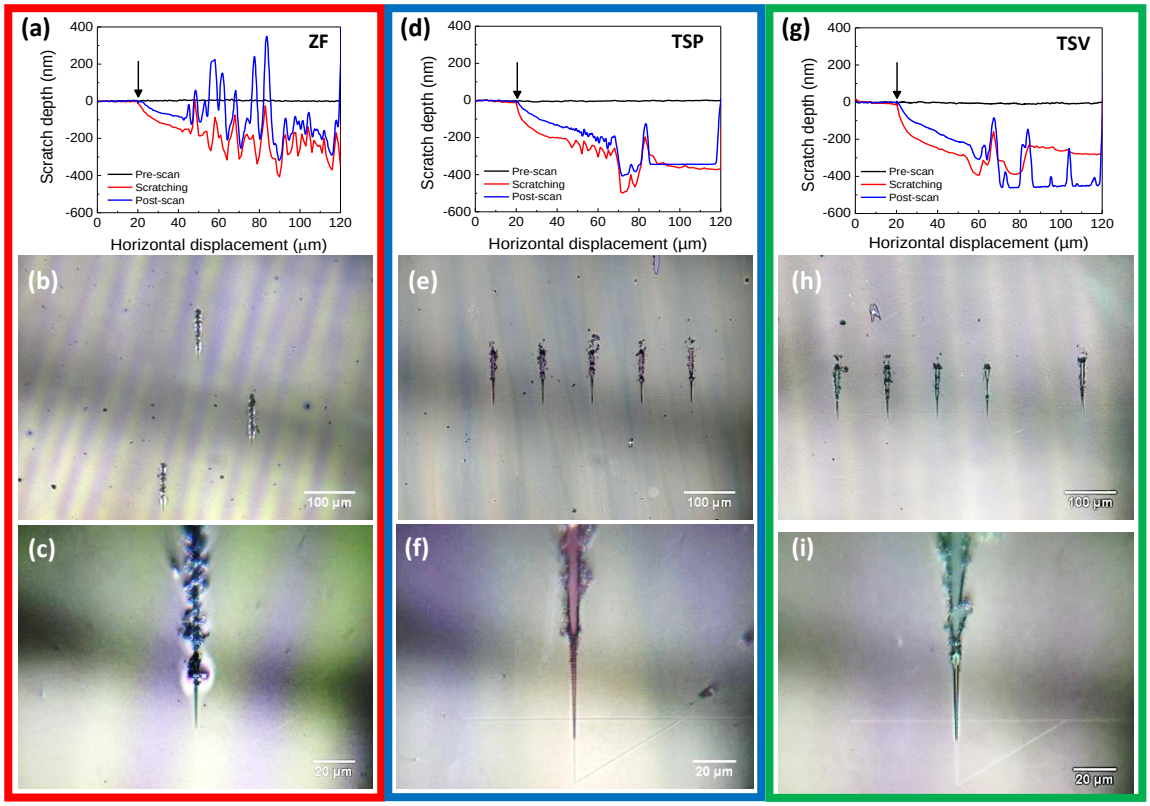

Figure S7. Scratch curves up to a maximum load of 5 mN for **(a)** ZF; **(b)** TSP and **(c)** TSV. Optical microscope images for the corresponding scratches: **(b,c)** ZF; **(e,f)** TSP and **(h,i)** TSV. The arrows indicate the beginning of the scratching.

5) Construction and detection properties of protected Tamm devices

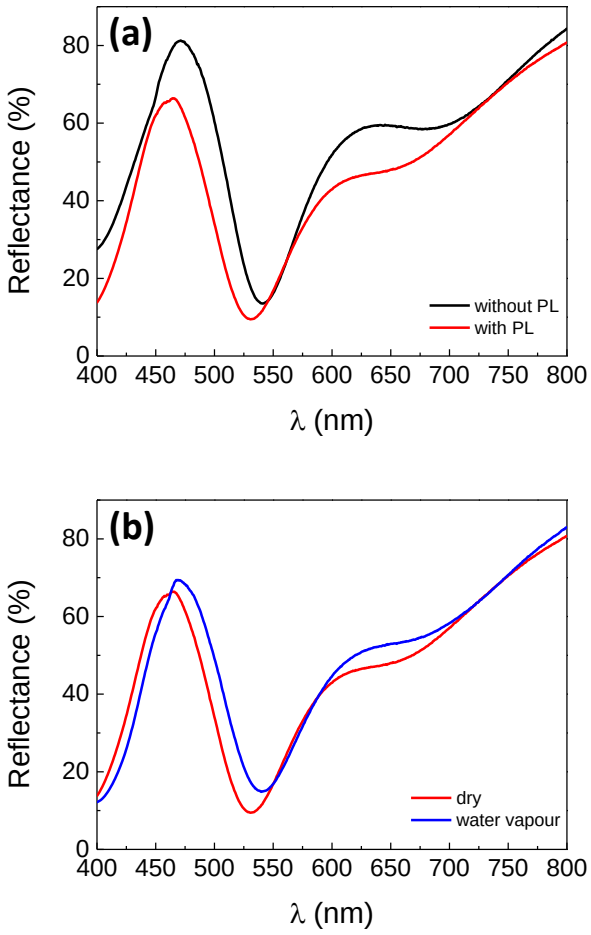

Figure S8. (a) Reflectance spectra of 4x(SB/TF)/Au and of the same device with ZF PL (4x(SB/TF)/Au/ZF). **(b)** Response to water vapour for 4x(SB/TF)/Au/ZF.

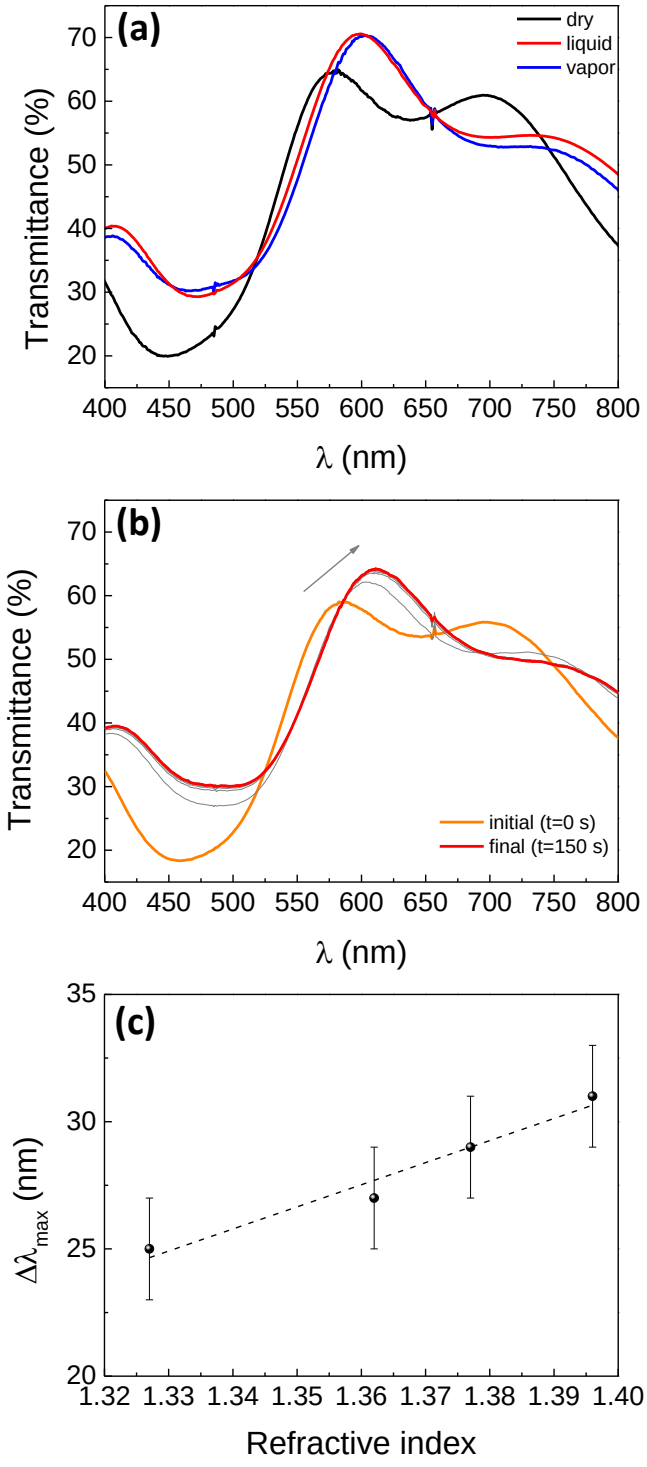

Figure S9. (a) Transmittance spectra of 4x(SC/TB)/Au/TSV measured dry, in an atmosphere saturated with butanol vapour and after immersion in liquid butanol. **(b)** Dynamic response of the same device in contact with liquid butanol. The orange curve corresponds to the initial state (dry, t= 0 s) and the red one to the final state (full of solvent, t= 150 s). **(c)** Linear calibration curve for the variation of the Tamm peak position of the protected device as a function of refractive index for different vapours (alcohols) filling the pores. The sensitivity of the device is (90±10) nm.RIU^{-1}.

References

1. M. C. Fuertes, F. J. López-Alcaraz, M. C. Marchi, H. E. Troiani, V. Luca, H. Míguez and G. J. A. A. Soler-Illia, *Adv. Funct. Mater.*, 2007, **17**, 1247-1254.
2. P. C. Angelomé, M. C. Fuertes and G. J. A. A. Soler-Illia, *Adv. Mater.*, 2006, **18**, 2397-2402.
3. B. Auguié, M. C. Fuertes, P. C. Angelomé, N. L. Abdala, G. J. A. A. Soler Illia and A. Fainstein, *ACS Photonics*, 2014, **1**, 775-780.
4. Z. Knittl, *Optics of Thin Films: An Optical Multilayer Theory*, Wiley, London, 1976.
5. B. Auguié, A. Bruchhausen and A. Fainstein, *Journal of Optics*, 2015, **17**, 035003.
6. P. B. Johnson and R. W. Christy, *Physical Review B*, 1972, **6**, 4370-4379.
7. W. C. Oliver and G. M. Pharr, *J. Mater. Res.*, 2011, **7**, 1564-1583.
8. R. B. King, *International Journal of Solids and Structures*, 1987, **23**, 1657-1664.